Invariant Image Reparameterisation: A Unified Approach to Structural and Practical Identifiability and Model Reduction

Oliver J. Maclaren[1], Ruanui Nicholson[1], Joel A. Trent[1], Joshua Rottenberry[2], and Matthew J. Simpson[2,3]

[1]Department of Engineering Science, University of Auckland, Auckland 1142, New Zealand.
[2]School of Mathematical Sciences, Queensland University of Technology (QUT), Brisbane, Australia.
[3]ARC Centre of Excellence for the Mathematical Analysis of Cellular Systems, QUT, Brisbane, Australia.

Abstract

Parameter non-identifiability – both structural and practical – presents a fundamental challenge when using mathematical models to interpret experimental or observational data and perform reliable uncertainty quantification. This issue is particularly acute in highly complex, applied areas such as the life sciences or engineering, where determining appropriate model complexity is complicated by experimental constraints and noisy data. While several approaches exist for diagnosing and resolving parameter non-identifiability, including symbolic/algebraic methods, profile likelihood analysis, and sloppiness analysis, these approaches have distinct limitations and are rarely combined. We present a novel integrated approach called Invariant Image Reparameterisation (IIR) that combines key elements of these methods to carry out both structural and practical identifiability analysis. Our approach enables the discovery and ordering of common classes of practically identifiable nonlinear parameter combinations without

1

requiring symbolic computation. This goal is achieved through a sloppiness-inspired log coordinate transformation that enables the replacement of symbolic reparameterisation computations with numerical calculation at a single reference estimate, and an invariance condition determines when this local calculation holds globally. The parameter combinations determined by this method are also naturally ordered by degree of identifiability. By treating these combinations as interest parameters within our established likelihood-based Profile-Wise Analysis framework, we further enable a unified analysis of nonlinear practical identifiability, model reduction, uncertainty quantification, and model-based prediction. To facilitate practical adoption, we provide open-source Julia software demonstrating our methodology across diverse mathematical models spanning data science, physics, engineering, chemistry, and biology.

Short title: Invariant Image Reparameterisation

Keywords: Mathematical model; Identifiability; Parameter estimation; Uncertainty quantification; Model reduction; Prediction.

1 Introduction

Mechanistic mathematical models encoding specific assumed or conjectured mechanisms are widely used for interpreting experimental and observational data and, hence, learning about underlying causes of the observed phenomena. Mathematical models are routinely used to provide insight into a broad range of applications including engineering (e.g. material science [1, 2], fluid dynamics and transport [3, 4]), ecology and population biology [5], disease transmission dynamics [6] as well as chemical reactions [7] and econometrics [8], among many other application areas. Regardless of the application area, an essential challenge in this undertaking is determining whether a particular measurement design and corresponding datasets contain enough information to give unique or sufficiently precise model parameter estimates. Parameter estimates are of interest both as representations of underlying mechanisms and as an intermediate step in constructing further predictions beyond the sample data.

Establishing whether model parameters are uniquely determined is often referred to as *structural identifiability analysis* in the modelling literature [9, 10, 11, 12, 13, 14], and is also simply referred to as identifiability analysis in the statistical literature [15]. In contrast, learning whether sufficiently precise parameter estimates are possible when working with finite noisy observations corresponds to the notion of *practical identifiability* (or estimability) analysis [16, 15, 17, 18]. Parameter non-identifiability essentially means that several distinct combinations of parameters can replicate the same model outputs or observations, meaning that the mechanisms encoded in the mathematical model have not been uniquely determined by the observations [15, 19]. From an applications point of view, parameter non-identifiability can mean that different combinations of mechanisms in the mathematical model can explain the same data. The common situation of having parameter non-identifiability means that it is difficult to draw conclusions about which particular mechanisms explain observational phenomena.

When model parameters are not identifiable, we may wish to explore whether some particular combinations of parameters are nevertheless identified [15, 20, 21], as well as the related possibility of carrying out *model reduction* to simplify the model in some sense so that the resulting model is identified (i.e., has identifiable parameters) [12, 13]. We consider this task and its relation to identifiability analysis in the present work. A straightforward example of non-identifiability arises when we consider the spatial motion of invasion fronts of a biological population modelled by the well-known Fisher-Kolmogorov model [6]. In this reaction-diffusion model, individuals are assumed to undergo random migration with diffusivity D

and logistic proliferation with rate λ. Making the most straightforward observations of the long-time front velocity c enables us to estimate the product $D\lambda$ [22], since we have $c = 2\sqrt{D\lambda}$ for initial conditions with compact support [6, 23]. This data, however, provides no insight into estimates of D or λ individually since there are infinitely many choices of D and λ that give rise to the same long-time speed of invasion. This non-identifiability means that making observations of the travelling wave speed c does not provide specific mechanistic insight into the rate at which cells move or rate at which cell proliferate.

Many approaches have been used to determine the identifiability of parameter combinations in the presence of non-identifiability (whether practical or structural) of the complete model parameter set. In the literature the main methods include: (i) symbolic/algebraic structural identifiability methods [24, 20, 25]; (ii) profile likelihood practical identifiability methods [26, 27, 28, 29, 30, 31, 32, 33]; and, (iii) model sloppiness analysis [34, 35, 36, 37]. Each approach brings certain strengths and limitations. For example, symbolic methods excel at automatically suggesting identifiable parameter combinations [20, 21] but typically directly apply only to structural identifiability problems and idealised infinite noise-free data which means that the results are not always applicable to real-world scenarios with sparse, imperfect data. Furthermore, when dealing with e.g. continuous state-space models, these methods typically require the use of Taylor or lie derivative series to generate exhaustive summaries of the model output (see [20, 21] for unified summaries of symbolic/algebraic methods and the role of different methods of generating the required exhaustive summaries). Alternatively, statistical likelihood-based methods excel at handling practical identifiability and providing estimates of uncertainty [38] but usually require user choices of interest parameter combinations to analyse, which means that automation is difficult. Finally, sloppiness analysis [34, 35, 36, 37] suggests identifiable parameter combinations in the practical identifiability setting but typically uses inaccurate and non-parameterisation-invariant approximations of cost or likelihood functions for uncertainty estimates. Furthermore, the relationship between sloppiness and identifiability is not always clear, as sloppiness is a relative notion quantified in terms of ratios of eigenvalues (or singular values) and, e.g., we may have a sloppy yet identifiable model [10].

A lack of full identifiability in a model generates a need and desire to reduce or reparameterise models using identifiable parameter combinations. These tasks – determinining identifiable combinations of model parameters and model reduction – are thus closely related. In applications of sloppiness and profile likelihood analysis to model reduction, users often simply set poorly-identified parameters to zero or some arbitrary value [39, 40, 41]. However, unless done carefully, this can lead to setting individually poorly-identified parameters to values

that jointly violate the requirements on possible values for the well-identified parameter combinations. For example, in the case of $c = 2\sqrt{D\lambda}$ discussed above, although D and λ are not identified from c, we cannot simply set one to e.g. zero unless this is consistent with what we know about c; the parameters appearing in a given combination must still satisfy some relationships jointly. Symbolic methods aim to systematically provide a model reduction based on a lower-dimensional reparametrisation [20, 21]. However, this requires explicit symbolic expressions for the model and the reparameterised reduced model, which may not be feasible for many mathematical or simulation models, and only covers structural non-identifiability for infinite noise-free data.

In this work we propose a new approach that: (i) automatically suggests well-identified parameter combinations without symbolic computation; (ii) implies reparameterisations suited to model reduction that does not require an explicit reduced form model; and (iii) collectively sets poorly-identified parameters in the original model consistently with well-identified parameter combinations, and provides interval estimates for both parameters and predictions with good statistical guarantees in the non-ideal data (practical identifiability/statistical analysis) setting. To achieve this, we present an approach for discovering practically identifiable parameter combinations consistent with the symbolic/algebraic literature but using parameter transformations inspired by the sloppiness literature to convert the general symbolic problem to a numerical problem that can be solved at a single reference estimate. We then use these parameter combinations as the interest parameters in our recently developed *Profile-Wise Analysis* (PWA) framework for practical identifiability, uncertainty analysis and model reduction based on profile likelihood [19, 38]. For certain general classes of identified parameter combinations, we can recover the information provided by structural methods up to essentially arbitrary accuracy. Outside of this exact class of parameter combinations, we can still discover approximate parameter combinations that facilitate more efficient prediction and estimation.

2 Methods

Here, we outline the technical foundations of our 'Invariant Image Reparameterisation' approach, which builds on and extends the frameworks reviewed in [20], [21], [38], and indirectly [15, 42]. Though we develop the details here and in the supplemental material TODO, a simple, practical algorithm for implementation is provided at the end of the section. We apply these methods to examples in the Results section.

Our method consists of four key components that work together to determine identifiable (and nonidentifiable) parameter combinations: (1) an auxiliary mapping that connects model parameters to observable quantities, (2) a general reparameterisation framework, (3) a coordinate transformation that simplifies the analysis and enables numerical computation, and (4) a singular value decomposition (SVD) for implementing the reparameterisation. Once identifiable (and nonidentifiable) parameter combinations are established, they can serve as so-called target or interest parameters in our Profile-Wise Analysis (PWA) workflow [38]. The last step could also be replaced by alternative approaches such as Bayesian inference, which can also benefit from reparameterisation methods CITE TODO.

Before presenting each component of our approach in detail, we first provide some essential mathematical background and notation.

2.1 Terminology

Throughout this section, we work relatively informally with (assumed-to-be) smooth mappings between finite-dimensional spaces and so recall some standard terminology (see, e.g., [43]). We assume the terms injective/one-to-one and surjective/onto mapping are known. In addition, a mapping is called a *submersion* if its derivative has full rank or, equivalently, if its derivative is an onto mapping into its target space. A mapping is called an *immersion* if its derivative is injective/one-to-one. Additionally, the *observed Fisher information*, which we use extensively, measures the amount of information data carries about parameters and is defined as the negative Hessian of the log-likelihood function [44, 32, 45]. The term *identifiable* refers to parameters or parameter combinations that can be uniquely determined from 'perfect data'. In the context of a model mapping parameters to data distributions, $\theta \mapsto p(y; \theta)$, this is equivalent to the mapping, or more generally an induced relation in terms of parameter combinations, being injective [15].

2.2 Model representation: the auxiliary mapping, exhaustive summaries, and data distribution parameters

We begin by representing the model structure through what we call [38] the auxiliary mapping ϕ, which connects model parameters to data distribution parameters that are assumed to be in one-to-one correspondence with the model data distribution. Though we use slightly different terminology, this is essentially identical to the 'exhaustive summary' approach re-

viewed by [20, 21]. This means we have a mapping of the form

$$\theta \mapsto \phi(\theta), \tag{1}$$

where θ are the mechanistic model parameters of the full model, along with a density function of the form

$$p(y; \phi), \tag{2}$$

where ϕ here provides a one-to-one parameterisation of possible density functions for observable data y. Together, these induce a probability model for data y given mechanistic model parameters θ:

$$p(y; \theta) = p(y; \phi(\theta)). \tag{3}$$

Here we are using the same symbol ϕ for both the mapping and the resulting data distribution parameter values. We assume that ϕ is known in terms of its role in parameterising data distributions, but the mapping $\phi(\theta)$ may only be known indirectly, e.g. through solving a differential equation or other mathematical model. For example, ϕ may represent the mean of a normal distribution, where this is, in turn, determined by solving a differential equation involving parameters θ. In the case where the data distribution parameters are formally infinite-dimensional, such as the solution to an ODE or PDE treated as the mean or related parameter of an observation model [46, 47], we consider ϕ to correspond to a finite-dimensional numerical approximation of the solution, such as a vector defined on a fine grid obtained from a numerical solver or simulation model. As we define our models in Julia, we can, relatively generally, evaluate any required derivatives using automatic differentiation/algorithmic differentiation at the source code level [48]. This is demonstrated in our two ODE examples. We thus avoid the need for alternative exhaustive summary methods such as Taylor series or generating series TODO REFs.

We also make use of the observed Fisher information (in various coordinates), which, in θ coordinates, is given by

$$\mathcal{J}(\theta) = -\mathrm{H}_l(\theta; y) = -\nabla_\theta (D_\theta l(\theta; y))^T = -\frac{\partial^2 l(\theta; y)}{\partial \theta \partial \theta^T} \tag{4}$$

where $l(\theta; y)$ is the log-likelihood of the model, i.e. $\log p(y; \theta)$ treated as a function of θ for fixed data y. Here, $D_\theta f = \frac{\partial f}{\partial \theta^T}$ denotes the Jacobian derivative of a function f with respect to θ, $\nabla_\theta f = (D_\theta f)^T$ denotes the gradient, and $H_f = \frac{\partial^2 f}{\partial \theta \partial \theta^T}$ denotes the Hessian [49]. We also use subscripts to denote differentiation when convenient, e.g. f_θ or $f_{\theta\theta}$, etc.

A central component of our approach is the observation that the above basic auxiliary mapping can always be decomposed as

$$\phi(\theta) = \tilde{\phi}(\psi(\theta)), \tag{5}$$

7

where:

- θ represents the original model parameters;

- $\psi(\theta)$ represents identifiable parameter combinations;

- $\tilde{\phi}$ provides a one-to-one mapping from identifiable parameter combinations to data distribution parameters;

We use a 'tilde' to denote the mapping ϕ written in terms of the (potentially reduced) identifiable parameter combinations. This function can be thought of as a reduced model taking just the identified parameter combinations. Our decomposition is illustrated in Figure 1.
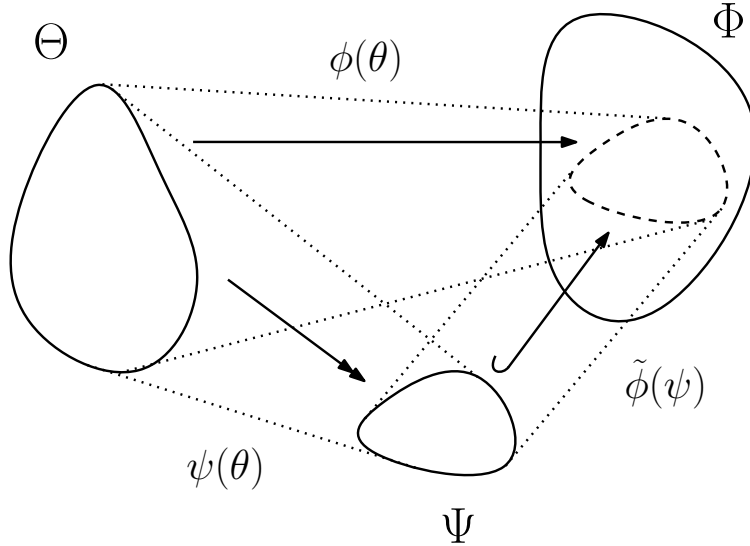

Figure 1: Illustration of the general decomposition of the auxiliary mapping into an identifiable reparameterisation followed by a reduced model mapping. Here θ represent the original model parameters, $\psi(\theta)$ represents identifiable parameter combinations, and $\tilde{\phi}$ provides a one-to-one mapping from identifiable parameter combinations to data distribution parameters. We use a double-headed arrow to indicate an onto mapping and an arrow with a hooked tail to represent a one-to-one mapping.

That such a decomposition is guaranteed to exist in principle, if not in practice, by the epi-mono factorisation property of the general category of sets and mappings [50], which states that any mapping $f : A \to B$ between sets A and B can be factored as the composition

$$f = m \circ e, \tag{6}$$

where $e : A \to C$ is onto (epimorphic), $m : C \to B$ is one-to-one (monomorphic), and C is some intermediate space, often called the *image*, $\mathrm{im}(f)$, in the context of category theory. That is, we have a factorisation of the form $A \to \mathrm{im}(f) \to B$. In standard set-theoretic definitions, the concrete subset of B determined as the output of $\mathrm{im}(f) \to B$ is often referred to as the image; here the intermediate space represents the basic 'abstract' image and the concrete realisation in B is determined up to a one-to-one embedding of this abstract image. This abstract factorisation can be thought of as a nonlinear generalisation of the rank factorisation in linear algebra CITE TODO; as discussed below, these ideas are even more closely related in the context of smooth, constant rank mappings (see, e.g. TODO REF). Such a decomposition is also at the heart of the prior approach of [20] and [21], though they do not state the result in this form and where what we call data distribution parameters they call exhaustive summaries of the model. The main contribution of our approach is an alternative, numerical method for constructing such decompositions. We consider this next.

2.3 Symbolic/algebraic reparameterisation condition

Here we provide our own, though essentially equivalent, presentation of the reparameterisation ideas discussed in [20, 21] TODO CATCHPOLE ETC TOO, where we emphasise that this approach provides a practical implementation of the general epi-mono factorisation ideas considered above. In particular, we can make progress beyond the general epi-mono factorisation structure by further assuming constant rank of ϕ and sufficient smoothness on all mappings involved.

Concretely, we assume that the epi-mono composition structure can be constructed such that $\psi(\theta)$ is a smooth submersion onto some intermediate manifold for all θ, and so $D_\theta \psi(\theta)$ has maximal rank for all θ and is surjective, and that $\tilde{\phi}(\psi)$ is a smooth immersion into the space of data distribution parameters, and so $D_\psi \tilde{\phi}(\psi)$ is injective for all ψ [43]. As above, D_θ denotes the Jacobian derivative with respect to θ, and similarly for ψ and so on.

Practically, these assumptions mean that the epi-mono factorisation structure is assumed to transfer to the corresponding composition of the derivatives arising from the chain rule. That is, given the composition structure above, we have, by the chain rule,

$$D_\theta \phi(\theta) = D_\psi \tilde{\phi}(\psi(\theta)) D_\theta \psi(\theta). \tag{7}$$

Under the above assumptions, the rank of $D_\psi \tilde{\phi}(\psi(\theta))$ and $D_\theta \phi(\theta)$ are the same as $D_\psi \tilde{\phi}(\psi(\theta))$ is one-to-one (see supplementary material TODO). Hence, when the overall ϕ mapping is

9

not one-to-one, we must have that the corresponding derivatives share the same null space (kernel), i.e.

$$\ker D_\theta \psi(\theta) = \ker D_\theta \phi(\theta). \tag{8}$$

Now, given explicit knowledge of $\phi(\theta)$ and $D_\theta \phi(\theta)$, this defines a differential equation to solve for $\psi(\theta)$. In particular, given null space vectors $\alpha(\theta)$ obtained from $D_\theta \phi(\theta)$, where $\alpha(\theta)$ are given as an explicit function of θ, we then solve

$$D_\theta \psi(\theta) \alpha(\theta) = 0, \tag{9}$$

for $\psi(\theta)$. Enforcing this for all and only the null-space vectors $\alpha(\theta)$, and requiring that the image of ψ is of dimension given by the rank of $D_\theta \phi(\theta)$, gives solution(s), not necessarily unique, for $\psi(\theta)$ defining an identifiable reparameterisation. This is equivalent to the conditions given by [20, 21] TODO CITE EARLIER WORK. It's also equivalent to equating the rows of $D_\theta \psi(\theta)$ to the vectors spanning the row space of $D_\theta \phi(\theta)$. The image of these vectors under ψ gives the intermediate 'image' component C of the epi-mono factorisation.

2.3.1   Fisher information formulation

The above is given in terms of the auxiliary mapping; as shown in detail in the supplementary material TODO REF, we can also work directly with the observed Fisher information, which provides an even closer link to practical identifiability concerns. This same point is discussed in [21]. Briefly, we assume that, as a function of the data distribution parameters, ϕ, with fixed data y, the log-likelihood $l(\phi; y)$ has a unique maximum in the interior of the mechanistically parameterised range, $\phi[\Theta]$, determined as the solution $\hat{\phi}$ to the first-order score equations $l_\phi(\phi; y) = 0$. We then call any mechanistic model parameter θ for which $\phi(\theta) = \hat{\phi}$ a maximum likelihood estimate of θ and denote it by $\hat{\theta}$, giving the following transformation law for the observed Fisher information:

$$\mathcal{J}(\hat{\theta}) = \phi_\theta(\hat{\theta})^T \mathcal{J}(\hat{\phi}) \phi_\theta(\hat{\theta}). \tag{10}$$

This transformation law of the observed Fisher information evaluated at the maximum likelihood is a well-known result $\phi(\theta)$ defines a one-to-one reparameterisation TODO REF but, as shown in the supplementary material, continues to hold even when ϕ is not one-to-one (as long as, essentially, the true data distribution can be obtained by some mechanistic model, i.e. $\phi_{\text{true}} \in \phi[\Theta]$).

Assuming the observed Fisher information, as considered in terms of data distribution parameters but not necessarily 'mechanistic' model parameters, is non-singular, the nullspace

and row space of the observed Fisher information are the same as that of the auxiliary mapping (supplementary material). This is a slightly stronger condition than assuming that the distribution parameters give a one-to-one indexing of the associated distributions but is a relatively weak assumption in general. We can thus alternatively determine the identifiable parameters by solving a nullspace constraint in terms of the Fisher information rather than the Jacobian derivative of the auxiliary mapping. We return to this below.

2.4   Parameter space linearisation and sloppiness

While the above condition provides a general approach to reparameterisation, it requires 'symbolic' or 'algebraic' knowledge of the Jacobian (or, equivalently, of the associated Fisher information) as a function of the mechanistic model parameter, and the null space we find is, hence, a function of the mechanistic model parameter. This is done by solving a partial differential equation. In contrast, numerical methods typically base analysis at a single point and only provide numerical values for null space vectors. This limits the reparameterisation information available to local reparameterisation or global but linear reparameterisations. Thus, numerical approaches are generally thought to be unable to provide meaningful non-linear reparameterisations of the type provided by symbolic methods [21]. However, here we show that we can apply an initial coordinate transformation to bridge these approaches. Importantly, as the likelihood function is invariant to reparameterisation [44, 32, 45], this approach loses no information; rather it aims to 'present' the information contained in the likelihood in a clearer form.

The parameter transformation we primarily focus on is the componentwise log transformation of all parameters, $\log \theta = [\log \theta_1, \log \theta_2, \ldots, \log \theta_p]^T$. However, our basic approach applies if, e.g. only some components are logged or even if both logged and unlogged parameters are considered simultaneously. In the context where each parameter is included only once in either logged or unlogged form, we can consider the parameters that aren't logged to be 'pre-logged' and the implicit 'original' parameters to be the exponentials of the logged parameters. The key assumption is that the coordinate transformation should be an immersion (i.e. have injective derivative). The motivation for focusing primarily on log transformations is that they are particularly natural for many physical and mechanistic models, where parameter combinations frequently appear as monomial dimensionless groups (so-called π terms) due to the Buckingham Pi theorem of dimensional analysis [51, 52].

While log-parameter transformations are commonly used in the sloppiness literature REF

TODO, and this inspired our present approach, the motivation for this choice is often not discussed in much detail in this literature beyond general reference to the idea that parameters in models typically span different orders of magnitude and that log transformations are related to working with dimensionless (and positive) parameters. Here, our motivation is explicitly that taking the log 'linearises' monomial terms in parameter space, though the overall function will still typically be a nonlinear function of the resulting linear combinations of log parameters. This turns out to be enough to reduce the reparameterisation condition to a single-point evaluation when the reduced parameter combinations are monomials.

Specifically, when parameters appear in the model in combinations of the form

$$\pi_i = \theta_1^{r_{i1}} \theta_2^{r_{i2}} \cdots \theta_p^{r_{ip}}, \tag{11}$$

where r_{ij} are typically integers in dimensional analysis, taking logarithms converts these nonlinear combinations into linear combinations:

$$\log(\pi_i) = r_{i1} \log(\theta_1) + r_{i2} \log(\theta_2) + \cdots + r_{ip} \log(\theta_p). \tag{12}$$

This means that if we define $\theta^* = \log(\theta)$ to be the *component-wise* log of the parameter vector, a model expressed in terms of parameter combinations such as dimensionless π groups can be written in the general form

$$\phi(\theta) = \tilde{\phi}(\exp(A\theta^*)), \tag{13}$$

where A is a matrix whose rows contain the coefficients r_{ij} and exp is the exponential function, similarly applied componentwise. Here $\tilde{\phi}$ is the one-to-one mapping appearing in the mono-epi factorisation introduced above. Note that $\exp A$ generates a vector of parameter combinations, each in the form of a monomial in the original parameters. Furthermore, if A has a null space, then the resulting vector $\exp(A\theta^*)$ can be of reduced dimension compared to θ^* and θ. While the coefficients in A are traditionally restricted to integers in dimensional analysis, here we allow them to be arbitrary real numbers to facilitate numerical computation and provide more flexibility in discovering practically useful parameter combinations. We also do not require the combinations to be dimensionless *a priori*. These relaxations come at a potential cost to interpretability, which we address later by considering scaling and rounding operations that can convert these real-valued coefficients to integers while preserving key properties of the approximation.

Writing the auxiliary mapping in terms of log parameters, i.e. defining $\phi_*(\theta^*) = \phi(\theta)$ and $\psi_*(\theta^*) = \psi(\theta)$, where we use an upper asterisk to denote logged variables, $\theta^* = \log \theta$, and we

use a subscript asterisk to indicate functions of the logged variables, the basic factorisation becomes:

$$\phi_*(\theta^*) = \tilde{\phi}(\psi_*(\theta^*)) \tag{14}$$

This idea is illustrated by the alternative pathway highlighted in Figure 2. We show a generic parameter transformation a in the figure to emphasise that while log transformation is the typical case, the idea applies more generally in principle.
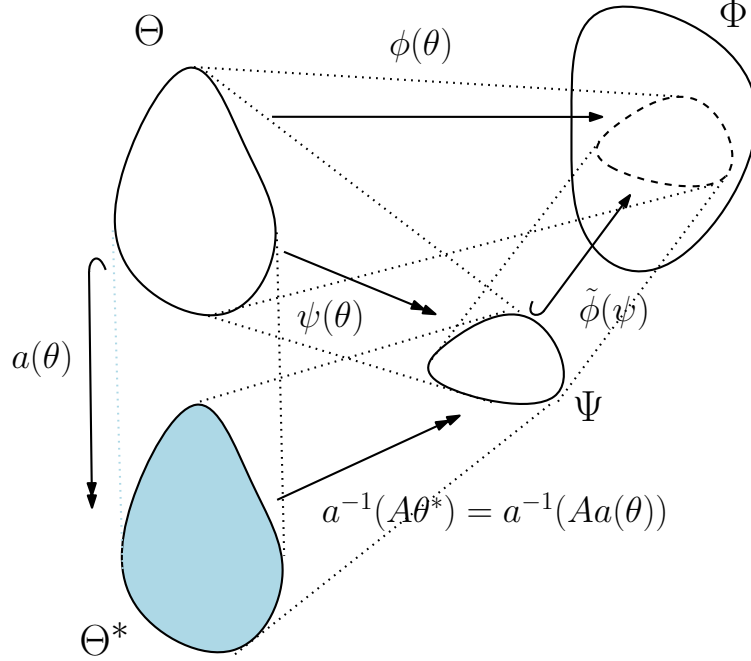

Figure 2: Illustration of the use of an initial componentwise transformation $a(\theta)$, typically log, followed by a linear transformation and a componentwise inverse, to generate identifiable parameter combinations. The chain rule applied on the path from Θ^* to Φ allows us to equate the overall null space to that of the constant linear transformation A, the key unknown of the parameter transformation.

The chain rule expression then becomes:

$$D_{\theta^*}\phi_*(\theta^*) = D_{\psi_*}\tilde{\phi}(\psi_*(\theta^*))D_{\theta^*}\psi_*(\theta^*), \tag{15}$$

where we have $\psi_*(\theta^*) = \exp(A\theta^*)$, and hence $D_{\theta^*}\psi_*(\theta^*) = \mathrm{diag}(\exp(A\theta^*))A$. Thus we have

$$D_{\theta^*}\phi_*(\theta^*) = D_{\psi_*}\tilde{\phi}(\psi_*(\theta^*))\mathrm{diag}(\exp(A\theta^*))A. \tag{16}$$

As $\tilde{\phi}$ is an immersion by our assumptions above, and the componentwise transformation a (typically exp) is also an immersion, their composition preserves the key properties of the

13

factorisation. In particular (see supplementary material for proofs), the first two terms in the chain rule equation compose to give an injective mapping, while the matrix A represents the potentially non-one-to-one, surjective linear mapping. This leads to our key condition defining the reparameterisation:

$$\ker A = \ker D_{\theta^*}\phi_*(\theta^*). \tag{17}$$

Here A is a (to be determined) constant matrix defining appropriate linear combinations of log parameters to generate monomials. Crucially, as the left-hand side is independent of the parameter value, the right-hand side must be as well; we can, therefore, evaluate the derivative at any convenient point and know the associated nullspace is the same globally. This reduces what would be a PDE in the original coordinates to an algebraic computation in logged coordinates. Once A is determined based on the above, following the procedure in the following subsection, we have determined our transformation given by equation 13. We note that the above does not uniquely determine A, but establishes the existence of such a matrix capturing the identifiable parameter combinations. As below, we choose a particular singular value decomposition approach to determine A, with further desirable properties, but other methods could be used.

If the model assumed non-identifiable, the point used will generally be, e.g., any (non-unique) maximum likelihood estimate, and the Jacobian will be singular. This is expected and causes no issues in general. We can evaluate the required derivative by finite differences or, in Julia in the cases we consider, by automatic/algorithmic differentiation of the source code [48]. Note that automatic differentiation at the source code level is distinct from symbolic differentiation and only evaluates the numerical value of the derivative at a fixed input value [53]. We also consider the case of near non-identifiability (i.e. practical non-identifiability) in the following subsections.

2.5 Singular value decomposition for nonlinear parameter combinations

The last main ingredient is a singular value decomposition of the Jacobian derivative in log-parameter coordinates to construct A and, hence, identify and separate parameter combinations based on their identifiability.

Specifically, given the Jacobian in log-parameters $D_{\theta^*}\phi_*$ at a reference estimate $\hat{\theta}^*$, we compute its SVD:

$$D_{\theta^*}\phi_*(\hat{\theta}^*) = U\Sigma V^T = U_r\Sigma_r V_r^T \tag{18}$$

where the second expression involving U_r, Σ_r and V_r is the reduced (cf. full) SVD, i.e. involving only non-zero singular values. The right singular vectors (columns of V) corresponding to non-zero singular values, i.e. those in V_r, span the space of locally identifiable parameter combinations, and the remainder span the non-identifiable parameter space. In particular, taking $A = V_r^T$, or any row-scaled version of this, ensures A has the same kernel (nullspace) as $D_{\theta^*}\phi_*(\hat{\theta}^*)$, and gives a reduced reparameterisation.

The case of practical identifiability, or near non-identifiability, is more subtle, but also handled by this approach. In this case, there will be singular values close to zero, and the corresponding singular vectors will be elements of the row space rather than the null space of the Jacobian. As the SVD leads to an orthogonal basis these singular vectors can still be considered to span a self-contained 'practically non-identifiable' parameter space, and the remaining singular vectors will still span the identifiable parameter space (there may also be a true null space if there are exactly zero singular values). The singular values thus provide a natural ranking of the identifiable parameter combinations by their 'degree of identifiability', including the possibilities of structural non-identifiability (zero singular value) and practical non-identifiability (small singular value). Treating the singular vectors as corresponding to parameter combinations with different degrees of identifiability rather than imposing a hard threshold somewhat avoids the issue of choosing a threshold and also leads to the idea of using a full reparameterisation, as discussed below.

2.5.1 Full reparameterisation

In the truly singular case, in addition to a reduced reparameterisation, we can also partition the full θ vector into identifiable combinations $\psi(\theta)$ and non-identifiable combinations $\lambda(\theta)$ using the full SVD via:

$$\theta \mapsto \begin{bmatrix} \psi(\theta) \\ \lambda(\theta) \end{bmatrix} = \exp(V^T \log(\theta)) \tag{19}$$

where $\phi(\theta)$ is the subvector corresponding to the rows of V^T associated with non-zero singular values and $\lambda(\theta)$ corresponds to the rows associated with zero singular values. This is useful because, although a model may in principle only depend on a reduced set of parameters, many simulation models are based on complex codes that take the full set of parameters as arguments and would have to be rewritten as functions of only the reduced set in order to run. By reparameterising the full set, including the non-identified parameters, the original codes can be used. Furthermore, as discussed above, in the case of near but not exact non-identifiability, i.e. practical non-identifiability, one would not want to accidentally

exclude potentially relevant variables based on some threshold. Given a log transformation, the combinations generated by the above take the form of products and ratios of original parameters to various powers.

2.5.2 Fisher information formulation

As mentioned above, since the nullspace and row space of the observed Fisher information are the same as that of the auxiliary mapping, we can also extend this approach to work directly with the observed Fisher information. This may be more natural for many models. Applying the same idea of an initial parameter-space linearising transformation, we can determine the identifiable parameters by solving a nullspace constraint, or, by simply considering the singular vectors (eigenvectors) of the Fisher information with non-zero singular values (eigenvalues). This is often the simplest approach in practice. If the parameters appear in monomial combinations in the nonlinear model, then an initial component-wise log transformation will enable us to find the identifiable parameters almost exactly, up to finite discretisation errors. Furthermore, the nullpace vectors define non-identifiable parameter combinations orthogonal to the identifiable combinations. Orthogonal parameters are particularly useful for likelihood-based statistical inference [54, 55], and we consider this aspect in more detail in the context of our results.

Following this approach, we again get a transformation (of the full parameter vector) of the form

$$\theta \mapsto \begin{bmatrix} \psi(\theta) \\ \lambda(\theta) \end{bmatrix} = \exp(\bar{V}^T \log(\theta)), \tag{20}$$

where $\bar{V}^T$ is now the matrix of singular vectors from the SVD of the observed Fisher information $\mathcal{J}(\theta^*)$ expressed in log-transformed coordinates θ^*.

2.6 Practical vs structural identifiability and observation operators

That the observed Fisher information and the auxiliary mapping have the same rank and null space may seem surprising at first, as the former is generally associated with *practical* identifiability analysis, while the latter is essentially a *structural* identifiability tool. However, recalling that we are taking the data distribution parameters ϕ to be given by the output of, e.g., a numerical simulation model, this is resolved by clarifying whether a given analysis is in terms of the solution grid resolution or the measurement grid resolution. That is, if

we consider our analysis at the level of our observation grid, then our mapping to data distribution parameters is actually given by, e.g.,

$$\phi = B_{\mathrm{obs}} \phi_{\mathrm{fine}} \tag{21}$$

where ϕ_{fine} is our fine-scale solution and B_{obs} is, e.g., a linear operator mapping the fine-scale vector to the vector of values at given observation points. This potentially introduces additional null space or at least additional poorly identified components. We can thus consider both structural and practical identifiability questions within the same framework, depending on whether we consider fine-scale discretisation or coarse-scale discretisation. If we consider our analysis on the ideal solution grid level, then, to numerical approximation, we will expect to obtain the same results as a structural identifiability analysis, though for ill-posed problems, it may be difficult or even impossible to distinguish effectively (i.e. practically) non-identified and truly (structurally) non-identified scenarios [15] TODO MORE REFs. In such cases we believe it is more appropriate to report the practical identifiability results, which is what the present approach provides.

A more subtle issue occurs when the 'poor identifiability' is not due to finite data issues as such, but rather due to the existence of a limiting approximate model involving a reduced set of parameters. That is, the existence of a structurally non-identifiable model in a particular parameter limit that is not exactly reached in reality. In this case, the auxiliary mapping (even on a 'fine grid'), can have arbitarily small singular values depending on the region of parameter space considered. This lack of clean division between practical and structural identifiability is discussed further in [15]. In the present work, our 'parameterised normal approximations to the binomial and Poisson models' example provides a simple illustration of this issue, where the limiting Poisson model is structurally non-identifiable, but the binomial model is only practically non-identifiable.

In practice, if we choose to normalise the rows of V^T to have integer entries where possible (by scaling and rounding rows appropriately) while maintaining orthogonality, the resulting parameter combinations should, in principle, correspond exactly to structurally identifiable (for non-zero singular values) and structurally non-identifiable (for zero singular values) combinations that would be found using symbolic methods. Furthermore, due to continuity of the singular vectors with respect to the singular values (REF TODO), in the case of near non-identifiability, the resulting parameter combinations should, depending on the rounding procedure used, typically correspond to those that are structurally identifiable and non-identifiable in the limit model where small singular values become zero. This is a key advantage of our approach, as it provides a bridge between numerical and symbolic methods

for structural identifiability analysis.

Although there exist various formal algorithms for determining integer or rational approximations to real-valued vectors (TODO REFs), here we use a simple scaling and rounding heuristic. Different scale factors for a given row reflect higher or lower powers of the corresponding basic combination of parameters and preserve orthogonality relationships and the key identifiability information. Rounding may break this slightly in some cases, but the effects are likely small in many cases, and attempts can be made to keep resulting vectors orthogonal. Scaling and rounding can be done by inspection or via automated heuristics (e.g. as in our Julia code), though we leave the best way to fully automate this to future work. In the case of structural non-identifiability, the effects of scaling and rounding can be reduced, as discussed above, by taking the grid considered to be the solution rather than the observation grid. The question of how reliably an approximating structurally non-identifiable model can be found in the practically non-identifiable case is a more open question. Though we consider this question in the context of our examples, we leave a more general analysis to future work.

Next, we describe a series of examples of varying complexity to which we will apply our methodology.

3   Example models

Here, we describe three examples of varying areas of application and complexity, covering statistics and data science (parameterised normal distributions based on approximations to the binomial and Poisson models) [56, 54, 57], biochemistry and bioengineering (Monod/Michaelis-Menten kinetics) [58, 59], and physics and engineering (groundwater modelling) [3].

3.1   Statistics and data science: Parameterised normal approximations to the binomial and Poisson models

Our first example is a 'toy' model motivated by the (seemingly) simple problem of simultaneously estimating the number of trials n and success probability p in a binomial model given a collection of independent success counts from repeating the n-trial experiment k of times, where k is known. This problem is reviewed in [56], where the authors note that the 'near

Poisson' regime of large n and small p lead to unstable maximum likelihood estimates. This corresponds to a non-identifiable limit and hence (as also shown here) a case of practical non-identifiability close to this limit. A likelihood-based analysis of the problem is given by [54], further discussed in [57], and our analysis of this example is inspired by theirs. To simplify the example, however, and to enable the use of derivative-based methods, we treat the 'number of trials' as a continuous parameter (similar ideas are used in modern higher-order likelihood theory [60]). In fact, although the binomial (and Poisson) models provide motivation for this example, here we treat the n and p parameters as simply providing an abstract parameterisation of the normal distribution model with a similar structure to more realistic mechanistic models. To further simplify the details of the example, we also consider a model analogous to the normal approximation of the binomial model, along with the associated Poisson limit.

With these caveats, the model we consider is, for a single experiment (each analogous to an 'n-trial' Binomial experiment):

$$Y \sim \mathcal{N}(np, np(1 - np)), \tag{22}$$

along with the 'Poisson limit' case:

$$Y \sim \mathcal{N}(np, np). \tag{23}$$

In our framework, this model is produced in a structured manner by combining the normal data distribution model, uniquely defined by the mean and variance parameters:

$$\begin{bmatrix} \mu \\ \sigma^2 \end{bmatrix} \leftrightarrow \mathcal{N}(\mu, \sigma^2), \tag{24}$$

with (for the non limiting model) the auxiliary mapping:

$$\phi : \begin{bmatrix} n \\ p \end{bmatrix} \mapsto \begin{bmatrix} np \\ np(1 - p) \end{bmatrix} = \begin{bmatrix} \mu \\ \sigma^2 \end{bmatrix}. \tag{25}$$

That is, the underlying (or 'mechanistic') parameter is given by vectors of the form

$$\begin{bmatrix} n \\ p \end{bmatrix}, \tag{26}$$

while the 'data distribution' parameters are the usual mean and variance parameters in one-to-one correspondence with a given normal distribution as in equation 24. The auxiliary

mapping defines the dependence of μ and σ^2 on the underlying parameters n, p. Although this is not really a 'mechanistic' model in the usual sense, one could consider an underlying binomial model is a lower-level mechanism that 'generates' the higher-level (approximately) normally distributed observations. The problem is to determine both n and p given k observations from the single experiment model given by equation 22 or 23.

3.2 Biochemistry and bioengineering: Monod/Michaelis-Menten kinetics

3.3 Physics and engineering: Groundwater modelling

4 Results and Discussion

4.1 Parameterised Normal Models

These examples are sufficiently simple that we can illustrate the core ideas analytically, and so we first consider some analytical results. These results are somewhat 'obvious' but we derive them according to our general framework to illustrate the method. Similarly, the numerical results we then discuss were produced without assuming these analytical results were available, and used our generic model-agnostic code.

We focus our analytical illustration on the Poisson limit model for simplicity, defined by equation 23. In this model we expect only np to be identifiable, as the variance is equal to the mean. We will show that both symbolic (original parameters) and numerical (log-transformed parameters) approaches obtain this result.

We also present the results of numerical, likelihood-based analysis of both parameterised normal models. We consider the likelihood functions in both original and our reparameterisations. Although the likelihood is invariant to reparameterisation, we see how the reparameterisation 'brings out' the separation of information concerning the identifiable and non-identifiable parameters. Furthermore, we see that approximate, non-parameterisation-invariant likelihood procedures such as quadratic log-likelihood approximations and likelihood 'slices' are more reasonable in the reparameterised space.

4.1.1 Analytical results: Poisson limit model, original parameterisation

To first obtain the symbolic result we note, as above, that the auxiliary mapping in terms of untransformed parameters is given by

$$\phi(n, p) = \phi(\begin{bmatrix} n \\ p \end{bmatrix}) = \begin{bmatrix} np \\ np \end{bmatrix}.$$

The Jacobian of this mapping is given by

$$D\phi(n, p) = \begin{bmatrix} p & n \\ p & n \end{bmatrix}. \tag{27}$$

This is a function of n and p and clearly has a non-trivial null space for all n and p. As the Jacobian and the associated null space depend on (are given as a function of) n and p we refer to this as the 'symbolic' null space of the model. We can determine this by inspection, noting that vectors of the form

$$\alpha(n, p) = \begin{bmatrix} n \\ -p \end{bmatrix} \tag{28}$$

satisfy $D\phi(n, p)\alpha(n, p) = 0$ for all n and p. Thus the symbolic null space has dimension one and is spanned by the vector $\alpha(n, p)$; furthermore, the row space of $D\phi(n, p)$ hence has dimension one and is spanned by a symbolic vector orthogonal to $\alpha(n, p)$. This implies that $\psi(n, p)$ is scalar-valued and can be determined by equating the (unknown) single row of $D\psi(n, p)$ to the (transpose of the) vector spanning the (known) row space of $D\phi(n, p)$. By inspection we see that the row space of $D\phi(n, p)$ is spanned by the vector

$$\begin{bmatrix} p \\ n \end{bmatrix}, \tag{29}$$

which is orthogonal to $\alpha(n, p) = [n, -p]^T$. These properties are also evident from the 'symbolic' rank factorisation of $D\phi(n, p)$:

$$D\phi(n, p) = \begin{bmatrix} p & n \\ p & n \end{bmatrix} = \begin{bmatrix} 1 \\ 1 \end{bmatrix} \begin{bmatrix} p & n \end{bmatrix}. \tag{30}$$

Thus we can determine $\psi(n, p)$ by solving the equations in the row space form

$$\frac{\partial \psi}{\partial n} = p$$
$$\frac{\partial \psi}{\partial p} = n, \tag{31}$$

or solving the partial differential equation

$$\frac{\partial \psi}{\partial n} n + \frac{\partial \psi}{\partial p}(-p) \tag{32}$$

based on the orthogonality of the rows of $D\psi(n, p)$ and the vectors spanning the null space of $D\phi(n, p)$.

By inspection we see that $\psi(n, p) = np$ is a solution to these equations, and hence the identifiable parameterisation is given by $\psi(n, p) = np$, as expected.

This approach is equivalent to that of [20, 21] but, as with their approach, requires symbolic determination of the Jacobian and the solution of partial differential equations. We now show how our numerical approach can determine the same result without symbolic manipulation. We can again carry out the key analysis analytically in this simple case.

4.1.2 Analytical results: Poisson limit model, log-transformed parameterisation

We now consider the Poisson limit model in log-transformed parameters. By definition (specifically, from parameterisation invariance) the auxiliary mapping in terms of log-transformed parameters satisfies

$$\phi_*(n^*, p^*) = \phi_*(\begin{bmatrix} n^* \\ p^* \end{bmatrix}) = \phi(\begin{bmatrix} n \\ p \end{bmatrix}) = \phi(\exp(\begin{bmatrix} n^* \\ p^* \end{bmatrix})), \tag{33}$$

where $n^* = \log n$ and $p^* = \log p$ and where exp is the componentwise exponential function so that

$$\begin{bmatrix} n \\ p \end{bmatrix} = \exp(\begin{bmatrix} n^* \\ p^* \end{bmatrix}).$$

The right-hand side of the above equation is obtained from the definition of the auxiliary mapping in terms of untransformed parameters:

$$\phi(\begin{bmatrix} n \\ p \end{bmatrix}) = \begin{bmatrix} np \\ np \end{bmatrix} = \begin{bmatrix} \exp(n^*)\exp(p^*) \\ \exp(n^*)\exp(p^*) \end{bmatrix} = \begin{bmatrix} \exp(n^* + p^*) \\ \exp(n^* + p^*). \end{bmatrix} \tag{34}$$

Thus the Jacobian of the auxiliary mapping in terms of log-transformed parameters is given by

$$D\phi_*(n^*, p^*) = \begin{bmatrix} \exp(n^* + p^*) & \exp(n^* + p^*) \\ \exp(n^* + p^*) & \exp(n^* + p^*) \end{bmatrix} = \exp(n^* + p^*) \begin{bmatrix} 1 & 1 \\ 1 & 1 \end{bmatrix}. \tag{35}$$

As expected, this takes the SVD form (up to normalisation of the singular vectors):

$$D\phi_*(n^*, p^*) = \underbrace{\underbrace{\begin{bmatrix} 1 \\ 1 \end{bmatrix}}_{D_{\psi_*}\tilde{\phi}(\psi_*(\theta^*))} \underbrace{\exp(n^* + p^*)}_{\text{diag}(\exp(A\theta^*))} \underbrace{\begin{bmatrix} 1 & 1 \end{bmatrix}}_{A}}, \tag{36}$$

where $\theta^* = [n^*, p^*]^T$, A is the matrix of the constant linear transformation component of the reparameterisation and $D_{\psi_*}\tilde{\phi}(\psi_*(\theta^*))$ is the Jacobian of the auxiliary mapping in terms of the transformed, identifiable parameters. The 'diagonal' matrix is a scalar in this case as the intermediate image is represented by a single parameter. Since $\psi_*(n^*, p^*) = \exp(n^* + p^*)$, and the output of the auxiliary mapping is

$$\phi_*(n^*, p^*) = \begin{bmatrix} \exp(n^* + p^*) \\ \exp(n^* + p^*) \end{bmatrix} = \begin{bmatrix} \psi_*(n^*, p^*) \\ \psi_*(n^*, p^*) \end{bmatrix}, \tag{37}$$

we have that $D_{\psi_*}\tilde{\phi}(\psi_*(\theta^*))$ is also constant in this case. In more general classes of models, the A matrix will remain constant, but the Jacobian of the auxiliary mapping in terms of the identifiable parameters will depend on the parameters.

Thus we conclude that the identifiable parameterisation is given by

$$\psi_*(n^*, p^*) = \exp(A\theta^*) = \exp\left(\begin{bmatrix} 1 & 1 \end{bmatrix} \begin{bmatrix} n^* \\ p^* \end{bmatrix}\right) = \exp(n^* + p^*) = \exp(\log n + \log p) = np. \tag{38}$$

This is the same result as obtained in the symbolic analysis above. However, as the A matrix here is constant, and corresponds (up to normalisation) to the singular vector of the Jacobian of the auxiliary mapping in log-transformed parameters, we can determine it with a single numerical evaluation of the Jacobian. This is the key advantage of our numerical approach.

We can also determine the non-identifiable parameters by considering the full SVD of the Jacobian (or by finding orthogonal vectors to the identifiable parameter combination). In this case, there is a single singular vector, given by (up to normalisation)

$$\begin{bmatrix} 1 \\ -1 \end{bmatrix}, \tag{39}$$

which spans the null space of the Jacobian and is orthogonal to the row space giving the identifiable parameter combination. This implies that the non-identifiable parameterisation is given by

$$\lambda_*(n^*, p^*) = \exp\left(\begin{bmatrix} 1 & -1 \end{bmatrix} \begin{bmatrix} n^* \\ p^* \end{bmatrix}\right) = \exp(n^* - p^*) = \frac{n}{p}. \tag{40}$$
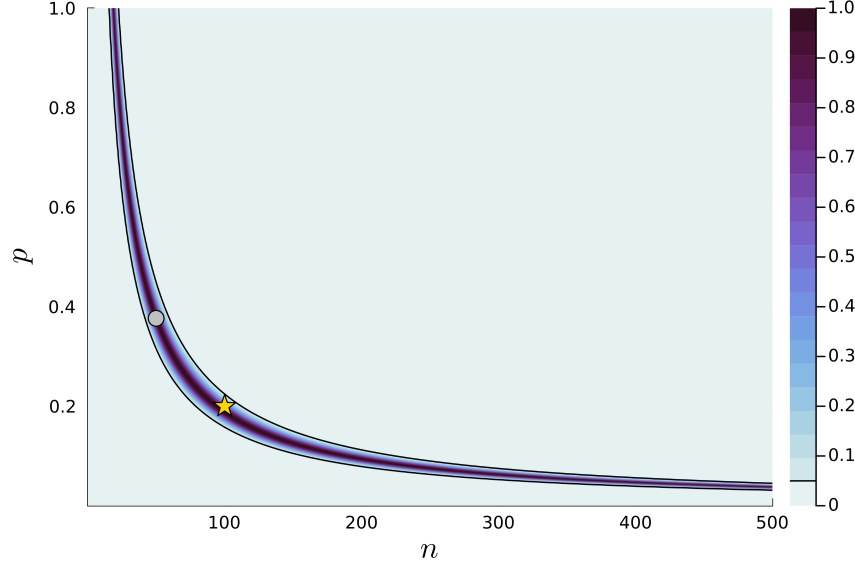
23

4.1.3 Numerical results: Poisson limit model

Below we present the results of our numerical analysis of the Poisson limit model. We consider the likelihood functions in both the original parameterisation, Figure 3, and the 'invariant image' reparameterisation, Figure 4. These results illustrate the separation of information concerning the identifiable and non-identifiable parameters in the reparameterised space, and the clearer suitability of approximate, non-parameterisation-invariant likelihood procedures in the reparameterised space.

In Figure 3, showing the likelihood in the original parameterisation, we see a long 'banana' shaped likelihood contour in the (n, p) plane, illustrating the existence of (approximately) equivalent parameter combinations lying along a curved relationship. The profile likelihoods for each parameter, shown in the bottom row of Figure 3, illustrate the individual non-identifiability of the parameters. The likelihood is completely flat for both parameters, other than where the bounds of the parameter space are reached. Together these results imply that the two parameters are not individually identifiable in this model, though there may be some combination of parameters that is identifiable (i.e. np, as we have shown analytically).

In Figure 4, showing the likelihood in the reparameterised space, we see the likelihood is constant in the vertical, $\frac{n}{p}$, direction and varies only in the horizontal, np, direction. This reflects the identifiability of the parameter combination np, and the non-identifiability of the parameter combination n/p. Furthermore this structure means the information concerning the identifiable and non-identifiable parameters is completely separated, as the likelihood factors into a product of a function of np and a (constant) function of n/p (see e.g. the discussion in [54, 55]). Thus we can, in principle, construct an autonomous reduced model based on the identifiable parameter combination np (as can be seen analytically).
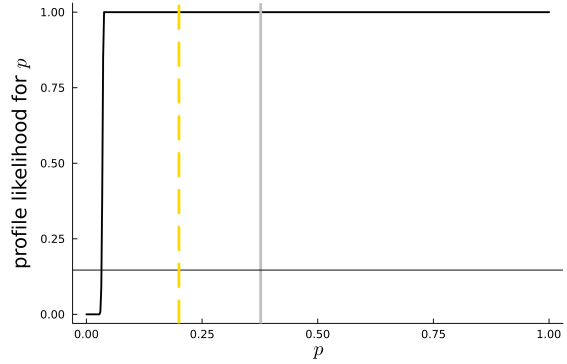
The profile likelihoods for each parameter, shown in the bottom row of Figure 4, further illustrate the distinct identifiability properties of the parameter combinations. The profile likelihood for np is a simple Gaussian-like function, showing good estimability, while the profile likelihood for n/p is completely flat, demonstrating non-identifiability. This is consistent with our analytical results.

(a) Joint likelihood contour plot in the (n, p) plane. The gold star indicates the true parameter value, and the silver circle indicates the maximum likelihood estimate. The colour bar represents the relative likelihood, with a black contour line indicating the 95% confidence interval threshold.
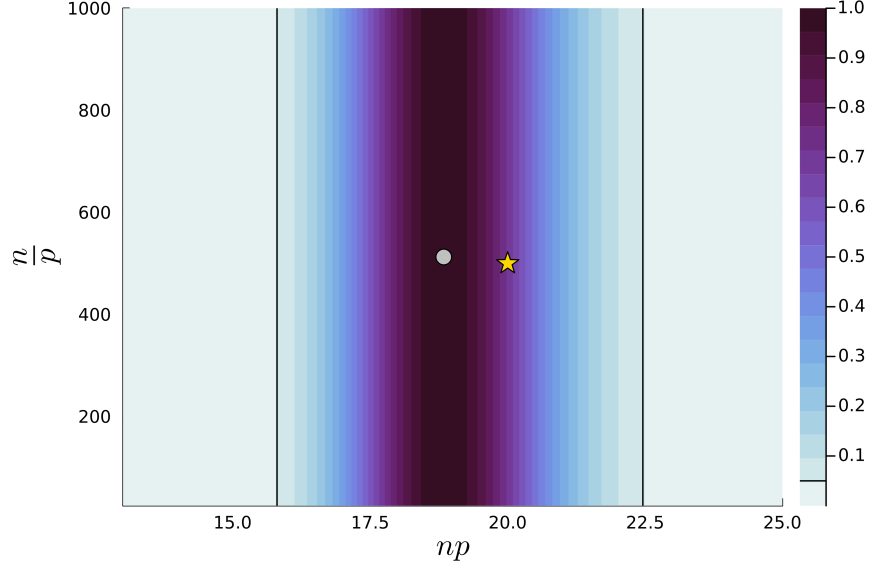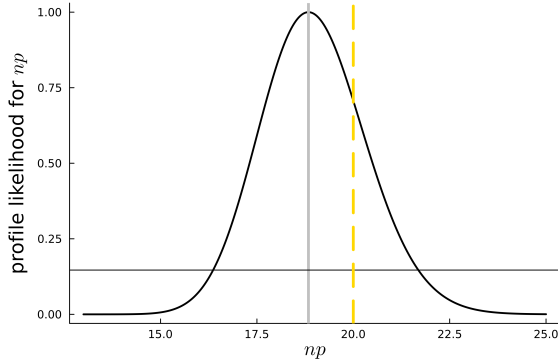

(b) Profile likelihood for n. The solid silver vertical line indicates the maximum likelihood estimate, and the dashed gold vertical line indicates the true parameter value. The horizontal black line indicates the threshold for the 95% confidence interval.

(c) Profile likelihood for p. The solid silver vertical line indicates the maximum likelihood estimate, and the dashed gold vertical line indicates the true parameter value. The horizontal black line indicates the threshold for the 95% confidence interval.
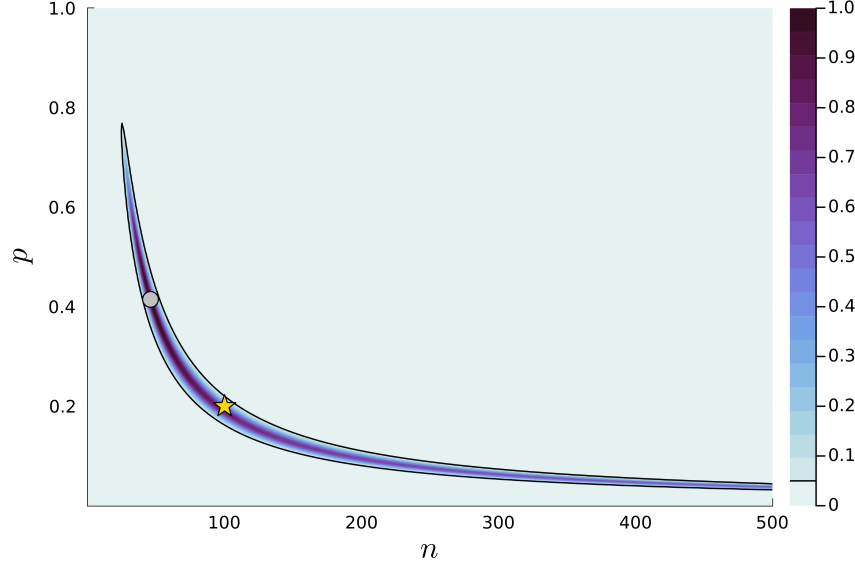
Figure 3: Poisson-limit example: (Top) joint contour in the (n, p) plane. (Bottom) profile likelihoods.

(a) Joint likelihood contour plot in the $(np, \frac{n}{p})$ plane. The gold star indicates the true parameter value, and the silver circle indicates the maximum likelihood estimate. The colour bar represents the relative likelihood, with a black contour line indicating the 95% confidence interval threshold.

(b) Profile likelihood for np. The solid silver vertical line indicates the maximum likelihood estimate, and the dashed gold vertical line indicates the true parameter value. The horizontal black line indicates the threshold for the 95% confidence interval.

(c) Profile likelihood for $\frac{n}{p}$. The solid silver vertical line indicates the maximum likelihood estimate, and the dashed gold vertical line indicates the true parameter value. The horizontal black line indicates the threshold for the 95% confidence interval.

Figure 4: Reparameterised Poisson-limit example: (Top) joint contour in the $(np, \frac{n}{p})$ plane. (Bottom) profile likelihoods.
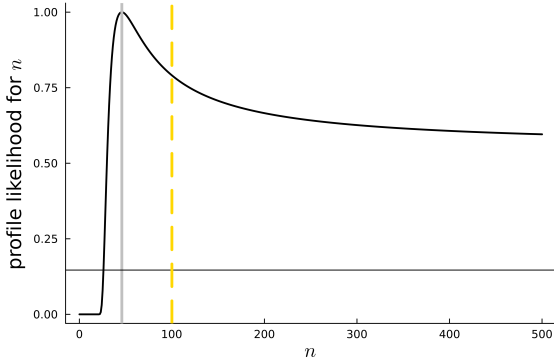
4.1.4 Numerical results: non-limit model

We now consider the non-limit model, defined by equation 22. As can be verified analytically, this model is now technically identifiable as long as we are not strictly in the Poisson limit. For example, the mean and variance are now distinct as $np \neq np(1-p)$ for $p \neq 0$, and we can solve for n and p separately from these two quantities. However, near the Poisson limit we also expect the parameters to be practically non-identifiable, i.e. poorly-identified. In this setting the well-identified parameter determined from the SVD will be close to np but not exactly equal to it, while there will be a poorly identified parameter close to n/p but not exactly equal to it. We can either work with the exact SVD singular vectors obtained e.g. for our point estimate or use the heuristic rounding approach to obtain the approximate reparameterisation (an alternative approach, not considered here but discussed later, is to evaluate the derivative in the limit regime and use the result in the non-limit regime). As long as the associated vectors are linearly independent, the reparameterisation is allowable and the associated (parameterisation-independent) likelihood analysis remains valid. The main difference is the extent to which exact or approximate separation of information is obtained and the extent to which the well-identified parameter is 'orthogonal' to the poorly-identified parameter, in the sense of observed Fisher-information orthogonality or in the sense of a likelihood factorisation (see e.g. [54, 55]). Here we find that our rounding heuristic indeed recovers the previous identifiable and non-identifiable parameter combinations as the implied reparameterisation, but that these now correspond to 'well-identified' and 'poorly but structurally identified' parameters, respectively.
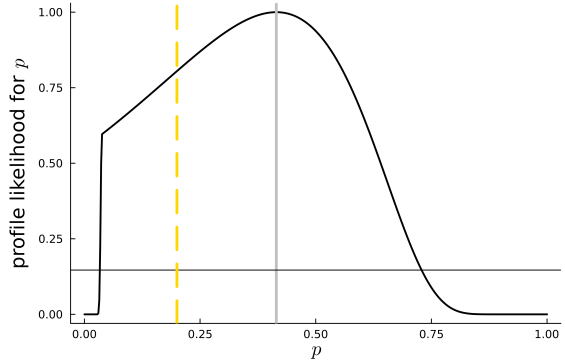
These results can be seen in Figures 5 and 6. These results largely mirror those of the Poisson limit model, with the well-identified parameter np and the poorly identified parameter n/p being clearly separated in the reparameterised space. However, in this case the separation is not exact, and the poorly identified parameter is not completely flat in the profile likelihood. We also see *one-sided identifiability* in both the original parameterisation and in the poorly identified parameter in the reparameterised model – the likelihood is much flatter on one side of the maximum likelihood estimate than the other. This is presumably due to the limit nature of the non-identifiability, i.e. that the model becomes poorly identified as we approach the Poisson limit, which occurs asymmetrically in parameter space. Overall, these results are consistent with the near non-identifiability of the parameters in this model, particularly in the Poisson limit.

(a) Joint likelihood contour plot in the (n, p) plane. The gold star indicates the true parameter value, and the silver circle indicates the maximum likelihood estimate. The colour bar represents the relative likelihood, with a black contour line indicating the 95% confidence interval threshold.
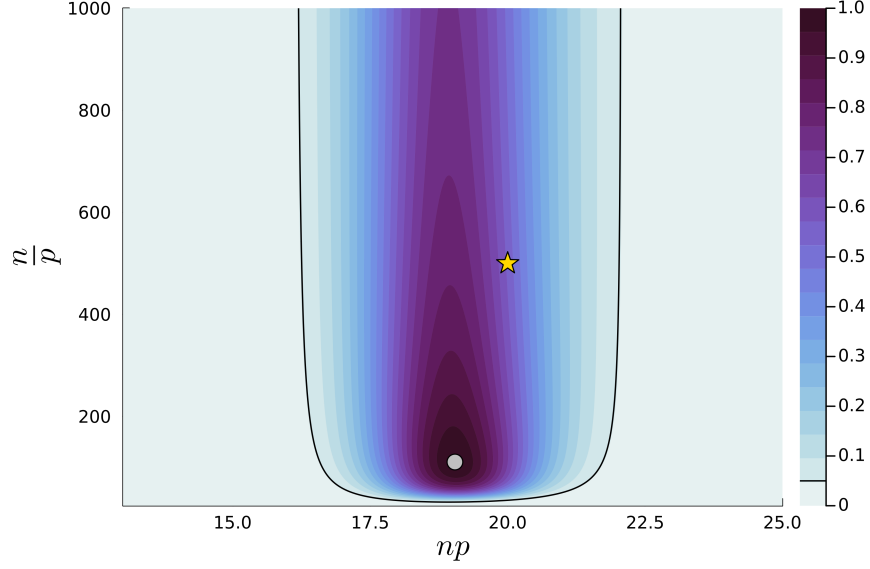

(b) Profile likelihood for n. The solid silver vertical line indicates the maximum likelihood estimate, and the dashed gold vertical line indicates the true parameter value. The horizontal black line indicates the threshold for the 95% confidence interval.
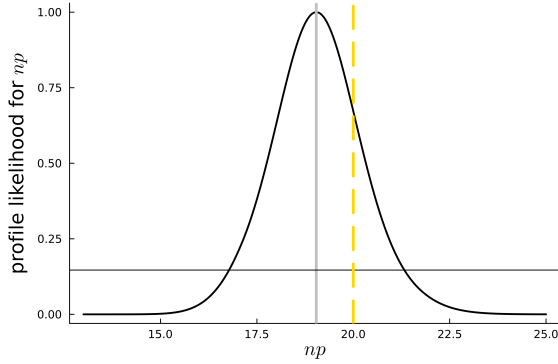
(c) Profile likelihood for p. The solid silver vertical line indicates the maximum likelihood estimate, and the dashed gold vertical line indicates the true parameter value. The horizontal black line indicates the threshold for the 95% confidence interval.
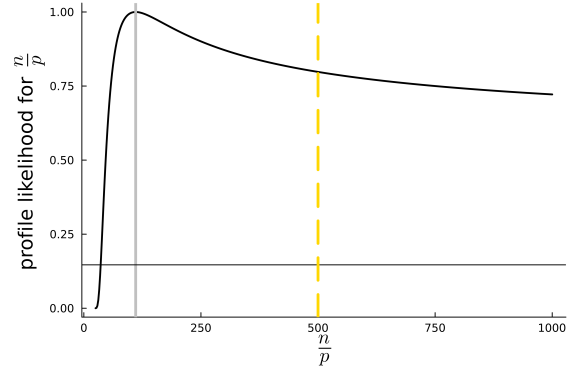
Figure 5: Non-limit (approximate Binomial) example: (Top) joint contour in the (n, p) plane. (Bottom) profile likelihoods.

(a) Joint likelihood contour plot in the $(np, \frac{n}{p})$ plane. The gold star indicates the true parameter value, and the silver circle indicates the maximum likelihood estimate. The colour bar represents the relative likelihood, with a black contour line indicating the 95% confidence interval threshold.

(b) Profile likelihood for np. The solid silver vertical line indicates the maximum likelihood estimate, and the dashed gold vertical line indicates the true parameter value. The horizontal black line indicates the threshold for the 95% confidence interval.

(c) Profile likelihood for $\frac{n}{p}$. The solid silver vertical line indicates the maximum likelihood estimate, and the dashed gold vertical line indicates the true parameter value. The horizontal black line indicates the threshold for the 95% confidence interval.

Figure 6: Reparameterised non-limit (approximate Binomial) example: (Top) joint contour in the $(np, \frac{n}{p})$ plane. (Bottom) profile likelihoods.

4.2 Monod/Michaelis-Menten kinetics

4.3 Groundwater modelling

5 Conclusion and Future Work

- Here we deal with ODE/PDE type models, but the concepts apply to SDE and simulation-based stochastic models too

- Here we deal with all parameters at once, but we can deal with subsets of parameters depending on our problem of interest.

6 Acknowledgements

7 Author Contributions

All authors contributed to the conceptualisation, review and editing of the manuscript. OJM wrote the original draft with contributions from MJS. Both OJM and MJS contributed to the choice of examples and design of numerical experiments. OJM developed the method details, proofs, wrote the code, and performed the numerical experiments, with discussion and input from the other authors.

8 Competing interests

The authors declare that they have no competing interests.

9   Data and materials availability

All data needed to evaluate the conclusions in the paper are present in the paper and/or the supplementary material. Julia code associated with this paper is available from GitHub.

References

1.   Gould PL and Feng Y. Introduction to Linear Elasticity. Springer, 2018

2.   Howell P, Kozyreff G, and Ockendon J. Applied Solid Mechanics. Cambridge University Press, 2008

3.   Bear J. Dynamics of Fluids in Porous Media. American Elsevier Publishing Company, 1972

4.   Krantz WB. Scaling Analysis in Modeling Transport and Reaction Processes. Wiley Interscience, 2007

5.   Kot M. Elements of Mathematical Ecology. Cambridge University Press, 2001

6.   Murray J. Mathematical Biology: I An Introduction. Springer, 2002

7.   Horn F and Jackson R. General mass action kinetics. Archive for Rational Mechanics and Analysis 1972; 47:81–116. DOI: 10.1007/BF00251225

8.   Hendry DF and Morgan MS. The foundations of econometric analysis. Cambridge University Press, 1997

9.   Bellu G, Saccomani MP, Audoly S, and D'Angió L. DAISY: A new software tool to test global identifiability of biological and physiological systems. Computer Methods and Programs in Biomedicine 2007; 88:52–61. DOI: 10.1016/j.cmpb.2007.07.002

10.   Chiş O, Villaverde AF, Banga JR, and Balsa-Canto E. On the relationship between sloppiness and identifiability. Mathematical Biosciences 2016; 282:147–61. DOI: 10.1016/j.mbs.2016.10.009

11.   Ligon TS, Frölich F, Chiş O, Banga JR, Balsa-Canto E, and Hasenauer J. GenSSI 2.0: multi-experimental structural identifiability analysis of SBML models. Bioinformatics 2018; 34:1421–3. DOI: 10.1093/bioinformatics/btx735

12. Meshkat N, Eisenberg M, and DiStefano III JJ. An algorithm for finding globally identifiable parameter combinations of nonlinear ODE models using Gröbner Bases. Mathematical Biosciences 2009; 222:61–72. DOI: https://doi.org/10.1016/j.mbs.2009.08.010

13. Meshkat N, Sullivant S, and Eisenberg M. Identifiability results for several classes of linear compartment models. Bulletin of Mathematical Biology 2015; 77:1620–51. DOI: 10.1007/s11538-015-0098-0

14. Díaz-Seoane S, Rey Barreiro X, and Villaverde AF. STRIKE-GOLDD 4.0: User-friendly, efficient analysis of structural identifiability and observability. Bioinformatics 2022; 39:btac748. DOI: 10.1093/bioinformatics/btac748

15. Maclaren OJ and Nicholson R. What can be estimated? Identifiability, estimability, causal inference and ill-posed inverse problems. arxiv preprint 2019; 1904.02826. DOI: 10.48550/arXiv.1904.02826

16. Hines KE, Middendorf TR, and Aldrich RW. Determination of parameter identifiability in nonlinear biophysical models: A Bayesian approach. Journal of General Physiology 2014; 143:401. DOI: 10.1085/jgp.201311116

17. Wieland FG, Hauber AL, Rosenblatt M, C T, and Timmer J. On structural and practical identifiability. Current Opinion in Systems Biology 2021; 25. DOI: 10.1016/j.coisb.2021.03.00

18. Kreutz C, Raue A, and J T. Likelihood-based observability analysis and confidence intervals for predictions of dynamics models. BMC Systems Biology 2012; 6. DOI: 10.1186/1752-0509-6-120

19. Simpson MJ and Maclaren OJ. Making predictions from nonidentifiable models. Bulletin of Mathematical Biology 2024; 86:80. DOI: 10.1007/s11538-024-01294-0

20. Cole DJ, Morgan BJT, and Titterington DM. Determining the parameteric structure of models. Mathematical Biosciences 2010; 228:16–30. DOI: 10.1016/j.mbs.2010.08.004

21. Cole D. Parameter redundancy and identifiability. CRC Press, 2020

22. Maini PK, McElwain DLS, and Leavesley DI. Traveling wave model to interpret a wound-healing cell migration assay for Human Peritoneal Mesothelial cells. Tissue Engineering 2004; 10:475–82. DOI: 10.1089/107632704323061834

23. Simpson MJ and McCue SW. Fisher–KPP-type models of biological invasion: open source computational tools, key concepts and analysis. Proceedings of the Royal Society A: Mathematics, Physics and Engineering Sciences 2024; 480:20240186. DOI: `10.1098/rspa.2024.0186`

24. Chappell MJ and Gunn RN. A procedure for generating locally identifiable reparameterisations of unidentifiable non-linear systems by the similarity transform approach. Mathematical Biosciences 1998; 148:21–41. DOI: `10.1016/S0025-5564(97)10004-9`

25. Chiş O, Banga JR, and Balsa-Canto E. Structural identifiability of systems biology models: a critical comparison of methods. Plos One 2011; 6:e27755. DOI: `10.1371/journal.pone.0027755`

26. Kreutz C, Raue A, Kaschek D, and Timmer J. Profile likelihood in systems biology. The FEBS Journal 2013; 280:2564–71. DOI: `10.1111/febs.12276`

27. Raue A, Kreutz C, Theis FJ, and Timmer J. Joining forces of Bayesian and frequentist methodology: a study for inference in the presence of non-identifiability. Philosophical Transactions of the Royal Society A: Mathematical, Physical and Engineering Sciences 2013; 271:20110544. DOI: `10.1098/rsta.2011.0544`

28. Raue A, Karlsson J, Saccomani MP, Jirstrand M, and Timmer J. Structural and practical identifiability analysis of partially observed dynamical models by exploiting the profile likelihood. Bioinformatics 2014; 30:1440–8. DOI: `10.1093/bioinformatics/btu006`

29. Villaverde AF, Raimúndez E, Hasenauer J, and Banga JR. Assessment of prediction uncertainty quantification methods in systems biology. IEEE/ACM Transactions on Computational Biology and Bioinformatics 2023; 30:1725–36. DOI: `10.1109/TCBB.2022.3213914`

30. Simpson MJ, Baker RE, Vittadello ST, and Maclaren OJ. Parameter identifiability analysis for spatiotemporal models of cell invasion. Journal of the Royal Society Interface 2020; 17. DOI: `10.1098/rsif.2020.0055`

31. Simpson MJ, Browning AP, Warne DJ, Maclaren OJ, and Baker RE. Parameter identifiability and model selection for sigmoid population growth models. Journal of Theoretical Biology 2022; 535:1100998. DOI: `10.1016/j.jtbi.2021.110998`

32. Pawitan Y. In all likelihood: statistical modelling and inference using likelihood. Oxford University Press, 2001

33. Maiwald T, Hass H, Steiert B, Vanlier J, Engesser R, Raue A, Kipkeew F, Bock HH, Kaschek D, Kreutz C, and Timmer J. Driving the model to its limit: Profile likelihood based model reduction. Plos One 2016; 11:e0162366. DOI: 10.1371/journal.pone.0162366

34. Brown KS and Sethna JP. Statistical mechanical approaches to models with many poorly known parameters. Physical Review E 2003; 68:021904. DOI: 10.1103/PhysRevE.68.021904

35. Brown KS, Hill CC, Calero GA, Myers CR, Lee KH, Sethna JP, and Cerione RA. The statistical mechanics of complex signaling networks: nerve growth factor signalling. Physical Biology 2004; 1:184. DOI: 10.1088/1478-3967/1/3/006

36. Gutenkunst RN, Waterfall JJ, Casey FP, Brown KS, Myers CR, and Sethna JP. Universally sloppy parameter sensitivities in systems biology models. PLOS Computational Biology 2007; 3:e189. DOI: 10.1371/journal.pcbi.0030189

37. Monsalve-Bravo GM, Lawson BAJ, Drovandi C, Burrage K, Brown KS, Baker CM, Vollert SA, Mengersen K, McDonald-Madden E, and Adams MP. Analysis of sloppiness in model simulations: unveiling parameter uncertainty when mathematical models are fitted to data. Science Advances 2022; 8:eabm5952. DOI: 10.1126/sciadv.abm5952

38. Simpson MJ and Maclaren OJ. Profile-Wise Analysis: A profile likelihood-based workflow for identifiability analysis, estimation, and prediction with mechanistic mathematical models. PLOS Computational Biology 2023; 19:e1011515. DOI: 10.1371/journal.pcbi.1011515

39. Lawrie J and Hearne J. Reducing model complexity via output sensitivity. Ecological Modelling 2007; 207:137–44. DOI: 10.1016/j.ecolmodel.2007.04.013

40. Elevitch CR and Johnson Jr CR. A procedure for ranking parameter importance for estimation in predictive mechanistic models. Ecological Modelling 2020; 419:108948. DOI: 10.1016/j.ecolmodel.2020.108948

41. Vollert SA, Drovandi C, Monsalve-Bravo GM, and Adams MP. Strategic model reduction by analysing model sloppiness: A case study in coral calcification. Environmental Modelling & Software 2023; 159:105578. DOI: 10.1016/j.envsoft.2022.105578

42. Maclaren OJ and Nicholson R. Models, identifiability, and estimability in causal inference. *Workshop on the Neglected Assumptions in Causal Inference (NACI) at the 38 th International Conference on Machine Learning, 2021.* 2021

43. Lee J. Introduction to Smooth Manifolds. Graduate Texts in Mathematics. Springer New York, 2013. Available from: `https : / / books . google . co . nz / books ? id = w4bhBwAAQBAJ`

44. Pace L and Salvan A. Principles of Statistical Inference from a Neo-Fisherian Perspective. World Scientific, 1997

45. Cox DR. Principles of statistical interence. Cambridge University Press, 2006

46. Murphy RJ, Maclaren OJ, and Simpson MJ. Implementing measurement error models with mechanistic mathematical models in a likelihood-based framework for estimation, identifiability analysis and prediction in the life sciences. Journal of the Royal Society Interface 2024; 21:20230402. DOI: `10.1098/rsif.2023.0402`

47. Simpson MJ, Murphy RJ, and Maclaren OJ. Modelling count data with partial differential equation models in biology. Journal of Theoretical Biology 2024; 580:111732. DOI: `10.1016/j.jtbi.2024.111732`

48. Revels J, Lubin M, and Papamarkou T. Forward-mode automatic differentiation in Julia. arXiv preprint arXiv:1607.07892 2016

49. Magnus JR and Neudecker H. Matrix differential calculus with applications in statistics and econometrics. John Wiley & Sons, 2019

50. Lawvere FW and Rosebrugh R. Sets for mathematics. Cambridge University Press, 2003

51. Buckingham E. On physically similar systems; illustrations of the use of dimensional equations. Physical review 1914; 4:345

52. Barenblatt GI. Scaling. Vol. 34. Cambridge University Press, 2003

53. Griewank A and Walther A. Evaluating derivatives: principles and techniques of algorithmic differentiation. SIAM, 2008

54. Aitkin M and Stasinopoulos M. Likelihood analysis of a binomial sample size problem. Contributions to probability and statistics: Essays in honor of ingram olkin 1989 :496–9

55. Cox DR and Reid N. Parameter orthogonality and approximate conditional inference. Journal of the Royal Statistical Society: Series B (Methodological) 1987; 49:1–18

56. Olkin I, Petkau AJ, and Zidek JV. A comparison of n estimators for the binomial distribution. Journal of the American Statistical Association 1981; 76:637–42

57. Aitkin M. Statistical inference: an integrated Bayesian/likelihood approach. CRC Press, 2010

58. Monod J. The growth of bacterial cultures. Annual Review of Microbiology 1949; 3:371–94. DOI: https://doi.org/10.1146/annurev.mi.03.100149.002103

59. Johnson KA and Goody RS. The original Michaelis constant: Translation of the 1913 Michaelis–Menten Paper. Biochemistry 2011; 50:8264–9. DOI: 10.1021/bi201284u

60. Davison AC, Fraser DA, and Reid N. Improved likelihood inference for discrete data. Journal of the Royal Statistical Society Series B: Statistical Methodology 2006; 68:495–508